Inclusion of Reactive Power into Ecological Robustness-Oriented Optimal Power Flow for Enhancing Power System Resilience

Hao Huang
Princeton University
hh6219@princeton.edu

H. Vincent Poor
Princeton University
poor@princeton.edu

Kate Davis
Texas A&M University
katedavis@tamu.edu

Abstract

Traditional optimal power flow problems focus on minimizing the operational cost, which can result in a fragile system during unexpected contingencies. An ecological robustness-oriented optimal power flow (R_{ECO} OPF) problem has been proposed to incorporate ecosystems' resilience characteristics into power system operations, enhancing their inherent resilience against multi-hazard contingencies. However, the original formulation of R_{ECO} only considered real power flows but neglected reactive power flows. In this paper, we include reactive power in the formulation of R_{ECO} and propose a reactive power flow based R_{ECO} OPF (Q-R_{ECO} OPF) and an apparent power flow based R_{ECO} OPF (MVA-R_{ECO} OPF) to guide the distribution of power flows, respectively. By comparing a 200-bus system's resilience against N-x contingencies using different OPF problems, we observe that both Q-based and MVA-based R_{ECO} OPF can provide a more resilient operating state.[1]

Keywords: Power System Resilience, Optimal Power Flow, Robustness, Ecosystems

1. Introduction

Power systems are the backbone of modern society, supplying electric energy for everyday activities. However, increasingly frequent unexpected events, including cyber attacks and natural disasters, have interrupted power systems' functionality and compromised their reliability, and thus threaten the security and safety of society. The U.S. National Academies' grid resilience report has specifically called for enhanced power system abilities to prepare for, endure, and recover from severe hazards National Academies of Sciences, Engineering, and Medicine (2017). Resilience has become a new requirement for modern power systems.

The U.S. Power Systems Engineering Research Center (PSERC) has recognized resilience as a system's capability to *gradually* deteriorate under increasing exertion and *rapidly* recover to its previous secure status Kezunovic and Overbye (2018) and Overbye et al. (2012). The distribution of power flows plays a critical role in determining power systems' inherent capability to maintain their security and reliability against contingencies, observed in the line overloads and voltage instability during contingencies. Traditionally, operators have used optimal power flows (OPFs) Cain et al. (2012) to operate power systems at their economic margins while meeting the operational requirements. To further ensure power systems' security and reliability, security constrained optimal power flows (SCOPFs) are employed to securely maintain a power system's functionality when one component is out of service Capitanescu et al. (2011).

As power systems have evolved into widespread cyber-physical systems, threats from cyber attacks, natural disasters, and extreme events can result in multiple components being simultaneously out of service, leading to catastrophic outcomes in power systems Shield et al. (2021) and Singer et al. (2022). To ensure power systems' resilience against such events, remedial actions and restoration preparations are essential. However, it is equally important to enhance the inherent resilience of power systems to limit the impact of disturbances, giving operators more time to take action and restore the system. Economic-driven

[1]Accepted for the 57th Hawaii International Conference on Science Sciences (HICSS),Honolulu, HI, January 2024; after the conference the paper will be available open access at https://hdl.handle.net/10125/39610

OPFs cannot satisfy the requirement of resilience for modern power systems.

An ecological robustness-oriented optimal power flow (R_{ECO} OPF) problem has been proposed to incorporate the long-term resilient characteristics of ecosystems into power flow distribution, thereby enhancing power systems' inherent resilience Huang et al. (2022). It uses R_{ECO} to guide a more robust distribution of power flows for enhanced inherent resilience, leading to fewer operational violations and unsolved contingencies when the system is subject to multiple hazards. However, the R_{ECO} OPF only considered real power flows for the formulation of R_{ECO} and did not consider the impact of reactive power flows no the system's robustness.

The planning and operation of reactive power are important. Unlike real power that is consumed as energy, reactive power serves the function of supporting and stabilizing the voltage of power systems. Optimal reactive power flow planning problems are formulated with different objectives, such as minimizing the voltage deviation, real power loss, and operational cost Zhang et al. (2007). Recent research has shown that strategically planning reactive power can also contribute to the enhancement of power systems' resilience against disruptions. Shaker et al. (2021) proposed a two-stage stochastic model to plan reactive power using networked microgrids against extreme events to reduce load shedding for better resilience. Kamruzzaman et al. (2021) proposed a multi-agent framework using deep reinforcement learning algorithms to plan the deployment of shunts for reactive power support, which enhances power system resilience with improved voltage stability against extreme events. Huang, Davis, et al. (2023) has investigated the use of reactive power flows and apparent power flows to formulate R_{ECO} for assessing power systems' resilience. The reactive power flow based R_{ECO} could better indicate power systems' resilience against *N-x* contingencies, necessitating the inclusion of reactive power into the formulation of R_{ECO} for assessing power systems' resilience. Thus, the research question raised in this paper is *"Can R_{ECO} be used to optimize the distribution of reactive and apparent power flows for enhancing power systems' inherent resilience?"*

This paper uses reactive power flows and apparent power flows to formulate R_{ECO} for the R_{ECO} OPF problem. Two new types of R_{ECO} OPF problems are proposed to enhance power systems' resilience through strategically guiding the distribution of reactive power flows and apparent power flows. The main contributions of this paper are as follow:

- With the inclusion of reactive power to formulate R_{ECO}, this paper introduces two new types of R_{ECO} OPF problems: reactive power based R_{ECO} OPF (Q-based R_{ECO} OPF) and apparent power based R_{ECO} OPF (MVA-based R_{ECO} OPF). They aim to enhance power systems' resilience through strategically distributing reactive and apparent power flows over the system, respectively.
- We apply both R_{ECO} OPF problems on the ACTIVSg200 system Birchfield et al. (2017) and investigate their impact on resilience under the examination of *N-1* and *N-2* contingencies. Both approaches improve the system's resilience resulting in fewer violations and unsolved contingencies as well as less severe contingencies, compared to OPF, SCOPF, and real power flow based R_{ECO} OPF (P-based R_{ECO} OPF) problems.
- Through analyzing the correlation among different types of power flow based R_{ECO}, power flow distribution, and the ACTIVSg200 system's resilience against *N-1* and *N-2* contingencies, we can observe that more homogeneously distributed real and reactive power flows contribute to the enhancement of a system's resilience.

2. Capturing Ecological Robustness in Power Systems

R_{ECO} is an information theory-based metric, leveraging topology of a food web to quantify its robustness. The input for calculating R_{ECO} is the ecological flow matrix ([**T**]), which captures the energy interactions within and across the system boundary for a food web. Figure 1 shows a hypothetical ecosystem and its conversion to [**T**]. The actors (species) that exchange energy based on a *prey-predator* relationship are within the system boundary, and the energy providers, energy export, and energy dissipation are placed outside of the system boundary Ulanowicz (2012). [**T**] is an (N+3) $\times$ (N+3) square matrix containing flow magnitudes of transferred energy over the system. *N* is the number of actors inside the system boundary, and the extra three rows/columns represent the system inputs, useful system exports, and dissipation. Energy flows in and out of an actor and the system are equal to maintain the *law of conservation of energy*.

The calculation of R_{ECO} originates from the concept of **surprisal** and **indeterminacy** Ulanowicz et al. (2009), which are expressed as

$$s = -k \times log(p) \tag{1}$$

where s is one's "surprisal" at observing an event that occurs with probability p, and k is a positive scalar

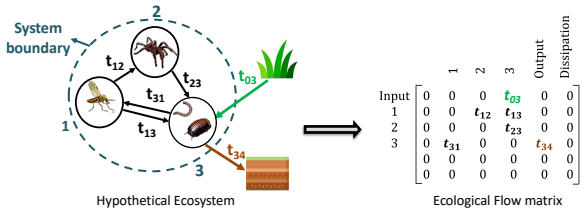

Figure 1. The conversion of a hypothetical ecosystem into an Ecological Flow Matrix.

constant. Throughout this paper, the value of k is 1.

$$h_i = -k \times p_i \times log(p_i) \tag{2}$$

where h_i is the indeterminacy of the event i. It is the product of the presence of an event p_i and its absence s_i, which measures the potential for change with respect to an event i.

Based on above concepts, R_{ECO} is formulated with following equations:

$$TSTp = \sum_{i=1}^{N+3} \sum_{j=1}^{N+3} T_{ij} \tag{3}$$

$$DC = -TSTp \sum_{i=1}^{N+3} \sum_{j=1}^{N+3} \left(\frac{T_{ij}}{TSTp} log_2 \left(\frac{T_{ij}}{TSTp} \right) \right) \tag{4}$$

$$ASC = -TSTp \sum_{i=1}^{N+3} \sum_{j=1}^{N+3} \left(\frac{T_{ij}}{TSTp} log_2 \left(\frac{T_{ij} TSTp}{T_i T_j} \right) \right) \tag{5}$$

$$R_{ECO} = -\left(\frac{ASC}{DC} \right) ln \left(\frac{ASC}{DC} \right) \tag{6}$$

where *TSTp* is the **Total System Throughput**, *DC* is the **Development Capacity**, and *ASC* is the **Ascendency**.

The *TSTp* is the sum of all flows in [**T**], capturing the system size. The *DC* is the aggregated maximum impacts (uncertainty) from all events (surprisals). The *ASC* is the aggregated impact of each flow updated with the knowledge of source and end nodes, and multiplied by the probability that the flow occurs in the first place Ulanowicz (1980), Ulanowicz et al. (2009), and Ulanowicz and Norden (1990). The ratio of *ASC* and *DC* reflects the *pathway efficiency* for a given network while its natural logarithm shows the network's *pathway redundancy*. R_{ECO} can thus quantitatively measure the robustness of ecosystems, which also represents the potential for food webs to continue functioning in the face of disturbances Ulanowicz et al. (2009).

Leveraging the similarity between ecosystems and power systems, previous works have modeled real power flows as energy transfer and power grid components (buses and generators) as analogous to food web species to formulate [**T**] and calculate R_{ECO}. Several R_{ECO} oriented optimization models have been proposed to optimize the power flow distribution and network structure to improve power systems' R_{ECO} with enhanced inherent resilience to survive from unexpected contingencies Huang et al. (2022), Huang, Mao, et al. (2023), and Panyam et al. (2019). However, power systems have a distinct feature regarding energy transfer, which is power flows consist of real and reactive power. Real power is the energy transferred and consumed within the system, while reactive power supports and stabilizes the system Glover et al. (2012). Power flows through the system combining both real and reactive power in a complex number form, $S = P + iQ$, known as apparent power. Real and reactive power are actually interrelated.

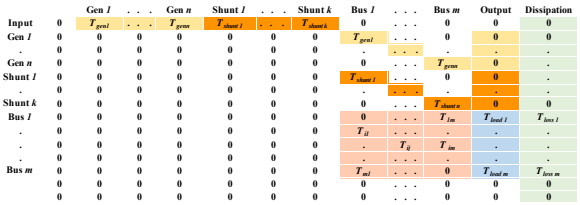

Figure 2. An extended Ecological Flow Matrix [T] for any type of power flows in a grid with n generators, k shunt capacitors, and m buses Huang, Davis, et al. (2023).

Even though power congestion attracts more attention for stakeholders due to economic losses, the voltage instability can cause cascading failures if there is insufficient reactive power planning. Huang, Davis, et al. (2023) extended the model of [**T**] with the consideration of *reactive power flow* and *apparent power flow* as well as shunt capacitors to comprehensively capture power systems' R_{ECO}. With a one-to-one mapping between power systems and ecosystems, Figure 2 presents a comprehensive model of [**T**] for any type of flow (T_{ij}) in power systems, which can be real power (P), reactive power (Q), or apparent power (MVA), respectively. T_{gen_i} is the flow from generator i, and T_{shunt_i} is the flow from shunt i. Since generators and shunt capacitors can either generate or consume reactive power, the corresponding entries in [**T**] can either be *Input* row or *Output* column based on the flow direction. T_{load_i} and T_{loss_i} are the power consumption and loss at Bus i, respectively. T_{ij} is the power flow at the corresponding branch from node i to j. If there is no power flow interaction among buses, shunts, and generators, the corresponding entry is zero. For apparent power flows, since the quantification of R_{ECO} cannot take complex numbers, the input of

apparent power flows is the magnitude and its direction is the same as its real power part.

3. Ecological Robustness-Oriented Optimal Power Flow

The objective of R_{ECO} OPF is to maximize the R_{ECO} of a given power system through adjusting the control variables of real (P_i) and reactive (Q_i) power injections, and bus voltages (magnitudes V_i and angles θ_i). It enhances power systems' inherent resilience with more a robust power flow distribution against unexpected hazards meanwhile satisfying power flow equations and power systems' operational limits. The problem is formulated as follows:

$$\text{Maximize } (R_{\text{ECO}} = g([\mathbf{T}])) \tag{7}$$

subject to

$$[\mathbf{T}] = f(T_{ij}, T_{gen_i}, T_{shunt_i}, T_{load_i}, T_{loss_i}) = \begin{bmatrix} 0, & T_{gen_i}, & 0, & ... & ... & 0 \\ 0, & ... & T_{gen_i}, & 0, & ... & 0 \\ 0, & ... & ... & ... & ... & 0 \\ 0, & ... & T_{ij}, & ... & T_{load_i}, & T_{loss_i} \\ 0, & ... & ... & ... & ... & 0 \\ 0, & ... & ... & T_{ij}, & T_{load_i}, & T_{loss_i} \\ 0, & ... & ... & ... & ... & 0 \end{bmatrix} \tag{8}$$

$$R_{ECO} = -\left(\frac{ASC}{DC}\right) ln\left(\frac{ASC}{DC}\right) \tag{9}$$

$$ASC = -TSTp \sum_{i=1}^{N+3} \sum_{j=1}^{N+3} \left(\frac{T_{ij}}{TSTp} log_2 \left(\frac{T_{ij} TSTp}{T_i T_j} \right) \right) \tag{10}$$

$$DC = -TSTp \sum_{i=1}^{N+3} \sum_{j=1}^{N+3} \left(\frac{T_{ij}}{TSTp} log_2 \left(\frac{T_{ij}}{TSTp} \right) \right) \tag{11}$$

$$TSTp = \sum_{i=1}^{N+3} \sum_{j=1}^{N+3} T_{ij} \tag{12}$$

$$v_i^l \leqslant V_i \leqslant v_i^u \ (\forall i \in \mathcal{M}) \tag{13}$$

$$s_{ij}^l \leqslant S_{ij} \leqslant s_{ij}^u \ (\forall (i,j) \in \mathcal{B}) \tag{14}$$

$$s_{gen_i}^l \leqslant S_{gen_i} \leqslant s_{gen_i}^u \ (\forall i \in \mathcal{G}) \tag{15}$$

$$S = P + iQ \tag{16}$$

$$P_{ij} = V_i^2[-G_{ij}] + V_i V_j [G_{ij} cos(\theta_{ij}) + B_{ij} sin(\theta_{ij})] \ (\forall (i,j) \in \mathcal{B}) \tag{17}$$

$$Q_{ij} = V_i^2[B_{ij}] + V_i V_j [G_{ij} sin(\theta_{ij}) - B_{ij} cos(\theta_{ij})] \ (\forall (i,j) \in \mathcal{B}) \tag{18}$$

$$P_i = P_{load_i} - P_{gen_i} = \sum_j P_{ij} \ (\forall j \in \mathcal{M}) \tag{19}$$

$$Q_i = Q_{load_i} - Q_{gen_i} = \sum_j Q_{ij} \ (\forall j \in \mathcal{M}) \tag{20}$$

$$P_{loss_i} = \frac{1}{2} \sum_j (P_{ij}^2 + Q_{ij}^2)/(B_{ij} V_i^2) \ (\forall j \in \mathcal{M}) \tag{21}$$

$$Q_{loss_i} = \frac{1}{2} \sum_j (P_{ij}^2 + Q_{ij}^2)/(G_{ij} V_i^2) \ (\forall j \in \mathcal{M}) \tag{22}$$

where $\mathcal{B}$, $\mathcal{M}$, and $\mathcal{G}$ are the sets of all branches, buses, and generators; v_i^l and v_i^u are lower and upper bound on the bus voltage magnitude; s_{ij}^l and s_{ij}^u are lower and upper bound on the branch limit; and $s_{gen_i}^l$ and $s_{gen_i}^u$ are lower and upper bound on the generator output, respectively.

Equations (7) states the objective of maximizing R_{ECO} given power system's [**T**]. Equation (8) represents the ecological flow matrix [**T**] as in Figure. 2. Equations (12)-(9) are the formulation of R_{ECO}. Equations (13) - (20) ensure satisfaction of power balance and power system operational constraints. Equations (21)-(22) represent the nodal real and reactive power losses aggregated from all connected branches, respectively.

In order to incorporate reactive power into R_{ECO} OPF, the entries for [**T**] are replaced with reactive power and apparent power, respectively. In this way, R_{ECO} OPF can strategically guide the distribution of reactive power flows and apparent power flows to enhance the system's resilience against contingencies. To distinguish different types of R_{ECO} OPFs, we term the real power flow based R_{ECO} OPF as P-based R_{ECO} OPF Huang et al. (2022), the reactive power flow based R_{ECO} OPF as Q-based R_{ECO} OPF, and the apparent power based R_{ECO} OPF as MVA-based R_{ECO} OPF, respectively.

4. Case Study

In this paper, we apply the Q-based and MVA-based R_{ECO} OPF problems to the ACTIVSg 200 system with both the quadratic-convex relaxation (QCLS) power flow model Sundar et al. (2018) and AC power flow model. R_{ECO} OPF problems are built with *PowerModels.jl* Coffrin et al. (2018), and the solver for the R_{ECO} OPF problem uses *Ipopt* Wächter and Biegler (2006) and *Juniper* Kröger et al. (2018).

As mentioned in Huang et al. (2022), the formulation of R_{ECO} involves several layers of logarithm functions, whose hard constraint is that their inputs must remain positive. However, the inputs for calculating R_{ECO} are the power flows, and their directions can be reversed during the solving process. A Taylor Series Expansion of the natural logarithm function is applied to relax R_{ECO}. Given $x > 0$

$$\ln(x) = 2\sum_{n=1}^{\infty} \frac{((x-1)/(x+1))^{(2n-1)}}{(2n-1)} \tag{23}$$

$$\log_2(x) = \frac{2}{\ln(2)}\sum_{n=1}^{\infty} \frac{((x-1)/(x+1))^{(2n-1)}}{(2n-1)} \tag{24}$$

which ensures the feasibility of solving R_{ECO} OPF problems using state-of-art solvers.

All R_{ECO} OPF problems have been successfully solved with the given solvers. The solution from the solver provides the vectors V_i, θ_i, P_{gen_i}, and Q_{gen_i} for all buses and generators. Due to the relaxation, we adapt the control vectors back to the system and solve it with the AC power flow model to determine the *exact* power flow distribution in the system. It should be noted here that the control vectors from the QCLS and AC power flow model of Q-based R_{ECO} OPF are the same. We also investigate the power flow distribution in traditional OPF and SCOPF, which consider *N-1* contingencies. Both OPF and SCOPF are solved with *PowerWorld Simulator* (available at http://www.powerworld.com). Then, we calculate the R_{ECO} with real, reactive, and apparent power flows for all variations of the ACTVISg200 system. Table 1 shows the comparison of operational cost, power flow model, P-based, Q-based, and MVA-based R_{ECO}.

It can be observed that the Q-based R_{ECO} is higher than the MVA-based and P-based R_{ECO} for all cases. Since real power flows dominate apparent power flows, the MVA-based and P-based R_{ECO} show a higher correlation. With the impact from reactive power flows whose value of R_{ECO} is high, the MVA-based R_{ECO} is higher than P-based R_{ECO}. The Q-based R_{ECO} OPF has the highest value of P-based and MVA-based R_{ECO} (0.25891 and 0.27658). Both Q-based and MVA-based R_{ECO} OPFs improve the P-based R_{ECO}. This was not achieved by the P-based R_{ECO} OPF that only considers the real power flow for the formulation of R_{ECO}. However, the traditional OPF achieves the highest Q-based R_{ECO} (0.32098), and none of R_{ECO} OPF problems improve the Q-based R_{ECO} for this system.

Table 1. Ecological Robustness of all Variations of ACTVISg200 Cases

Case	Operational Cost ($/hr)	Power Flow Model	P-based R_{ECO}	Q-based R_{ECO}	MVA-based R_{ECO}
Base Case	49000	AC	0.25777	0.32097	0.27614
OPF ⋆	48991	AC	0.25778	0.32098	0.27614
N-1 SCOPF	49000	DC	0.25777	0.32097	0.27614
P-based R_{ECO} OPF	51479	DC	0.25692	0.3167	0.27624
P-based R_{ECO} OPF	50265	QCLS	0.25778	0.31765	0.27590
P-based R_{ECO} OPF	50850	AC	0.25788	0.31756	0.27657
Q-based R_{ECO} OPF ⋆⋆	50165	QCLS	0.25891	0.31783	0.27658
Q-based R_{ECO} OPF ⋆⋆	50165	AC	0.25891	0.31783	0.27658
MVA-based R_{ECO} OPF	50165	QCLS	0.25890	0.31782	0.27658
MVA-based R_{ECO} OPF	50165	AC	0.25890	0.31782	0.27658

[1] ⋆: Highest P-based R_{ECO}.
[2] ⋆: Highest Q-based R_{ECO}.
[3] ⋆: Highest MVA-based R_{ECO}.
[4] : Numbers are round up

Figure 3 shows the plots of P-, Q- and MVA-based R_{ECO} against the homogeneity of power flow distribution for all variations of the ACTIVSg200 system. The homogeneity of power flow distribution is quantified by $\frac{Mean(flow)}{STD(flow)}$, where a smaller value indicates that the flows across the system are closer to each other. We separately analyze the generators' outputs, branches' power flows, and all power flows (including generators' outputs and branches' power flows) in the system respect to P-based, Q-based, and MVA-based R_{ECO} to further investigate their correlations. Overall, the P-based R_{ECO} is positively related to the homogeneity of power flow distribution. When power flows are more evenly distributed, the system has a higher value of P-based R_{ECO}. A similar pattern can be observed for MVA-based R_{ECO}, as real power flows dominate apparent power flows. However, the impact of reactive power flows discounted this positive correlation. In some situations, a more homogeneous distribution of power flows is associated with a lower value of MVA-based R_{ECO}, and vice versa. As for Q-based R_{ECO}, there is a negative correlation with the homogeneity of power flow distribution. Less

homogeneously distributed power flows can contribute to a higher value of Q-based R_{ECO}. It is possible that reactive power is typically distributed within local areas, making them locally robust and resulting in a higher value of R_{ECO} for the system. Meanwhile, the R_{ECO} OPF mathematically drives power flows to be more homogeneously distributed over the whole system. As a result, R_{ECO} OPFs may reduce the value of Q-based R_{ECO} but increase the value of P-based and MVA-based R_{ECO} with more homogeneously distributed power flows.

5. Resilience Analyses

In this paper, we investigate a series of *N-1* and *N-2* contingencies, considering outages of branch, generator, bus, and substation across all variations of the ACTIVSg200 systems. The outage of a bus and substation disconnects all connected devices (*N-k*), which can cause catastrophic impacts on system operations. The number of *violated contingencies*, *unsolved contingencies*, and *violations* under contingencies can indicate the system's inherent capability to tolerate disturbances while maintaining their functionality, which is recognized as the system's survivability. The lower number of *violated contingencies*, *unsolved contingencies*, and *violations* signifies a better level of survivability against disturbances, indicating a more resilient system. It should be noted that all contingency analyses are performed without remedial actions to examine the system's inherent resilience.

Figures 4 and 5 show the results of survivability for all cases under *N-1* and *N-2* contingencies. In the *N-1 Generator Contingencies* and *N-2 Generator Contingencies*, all variations of the ACTIVSg200 system have the same results. All cases are able to securely maintain their functionality under *N-1 Generator Contingencies*, and have 4 violations with 4 violated contingencies under *N-2 Generator Contingencies*. Thus, we do not include their graphical illustration here. Regarding *N-1 Contingencies*, a slight improvement on survivability can be observed with Q-based and MVA-based R_{ECO} OPFs, where the number of violations is reduced by 1 compared to OPF, SCOPF, and P-based R_{ECO} OPF. Significant improvement on survivability is observed for *N-2* contingencies. Under the *N-2 Branch Contingencies*, the Q-based and MVA-based R_{ECO} OPFs resolve 4 violated contingencies and 12 violations compared to the original system. Although the P-based R_{ECO} OPF has one less unsolved contingency, its violations are significantly more than other cases. Under *N-2 Bus Contingencies*,

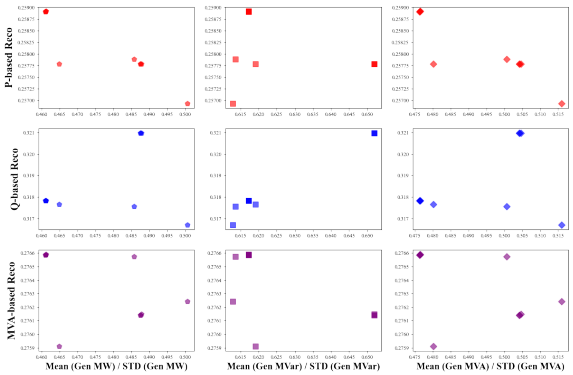

(a) Generators' Output

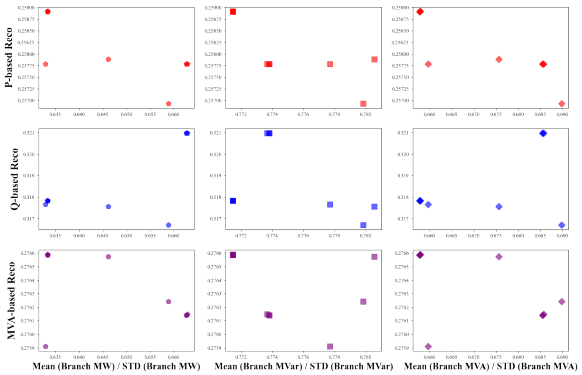

(b) Branch Flows

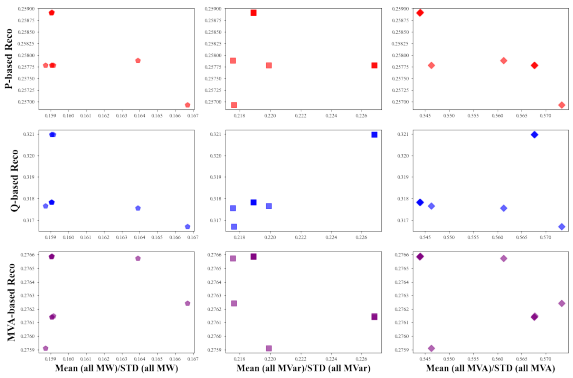

(c) All Flows

Figure 3. R_{ECO} v.s. Homogeneity of Power Flow Distribution.

the Q-based and MVA-based R_{ECO} OPF outperform all other cases with a reduction of 71 violations and 2 unsolved contingencies compared to the original system. Under the *N-2 Substation Contingencies*, the Q-based and MVA-based R_{ECO} OPFs also outperform other cases with a reduction of 8 violated contingencies, 87 violations, 5 unsolved contingencies. For *N-2*

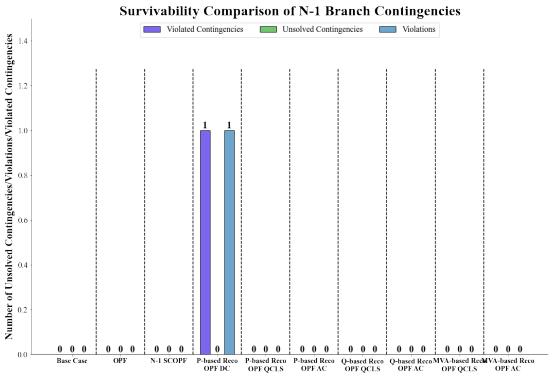

(a) N-1 Branch Contingencies

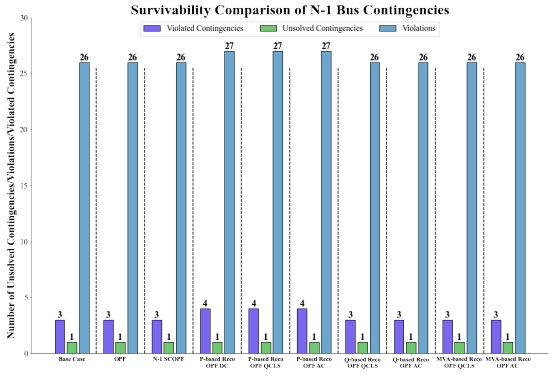

(b) N-1 Bus Contingencies

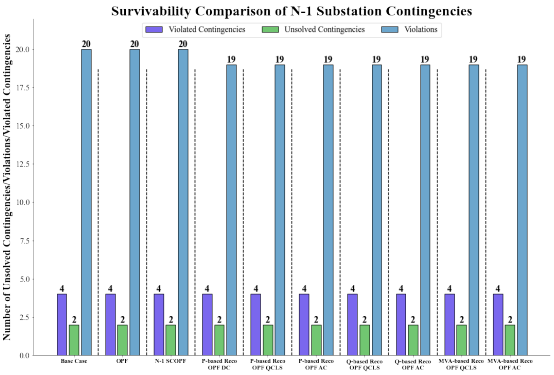

(c) N-1 Substation Contingencies

Figure 4. Survivability Comparison Under N-1 Contingencies

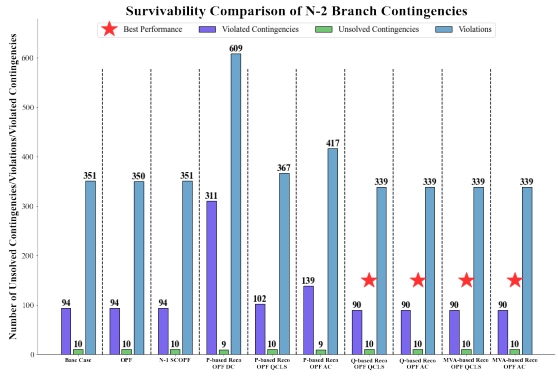

(a) N-2 Branch Contingencies

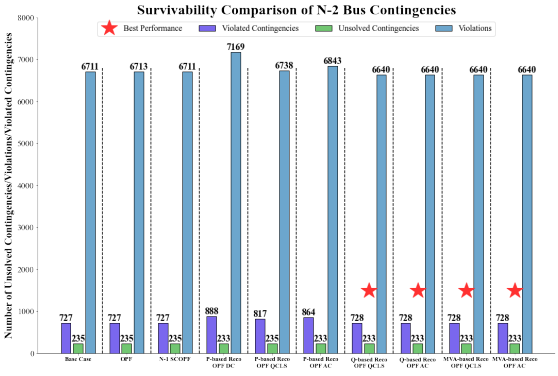

(b) N-2 Bus Contingencies

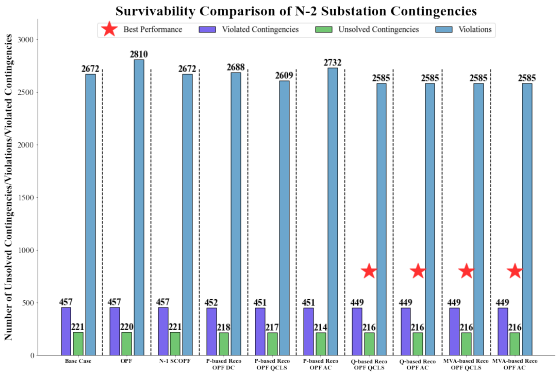

(c) N-2 Substation Contingencies

Figure 5. Survivability Comparison Under N-2 Contingencies

contingencies, the OPF and P-based R_{ECO} OPF have more violations.

As the number of violations are very close or the same for some cases, it is possible that the reduction on the number of violations may introduce more severe violations, which can cost more for operators to restore the system. Thus, we use an *impact factor* from Huang et al. (2019) to measure the severity of violated contingencies considering their overflows, under voltages, and over voltages to further investigate all cases' resiliency. This metric uses normalized values of voltage and power flow violations to quantify the impact of the contingency as shown in Equation (25). Since the voltage violation can be either over voltage or under voltage and the normal voltage p.u. is 1, the normalized value of a voltage violation impact is the absolute value of voltage instability minus 1. To equally

consider the impact of an overflow violation, Equation (25) uses the overflow percentage, which is over 100%, minus 1. The higher the impact factor is, the more severe violations happen in the system.

$$Impact\ Factor = \sum(overflow\ percentage - 1) + \sum abs(voltage\ instability - 1) \quad (25)$$

Table 2. Impact Factors of all Variations of ACTVISg200 Cases Under Contingency Analysis

Case Name	N-1 Bus Contingencies	N-1 Substation Contingencies	N-2 Branch Contingencies	N-2 Bus Contingencies	N-2 Substation Contingencies
Base Case	2.8712	2.2943	62.2886	901.1117	375.3804
OPF	2.8712	2.2990	62.3070	901.2186	398.3742
N-1 SCOPF	2.8712	2.2943	62.2886	901.1117	375.3804
P-based Reco OPF DC	2.9832	2.1867	81.9206	984.7622	397.7063
P-based Reco OPF QCLS	2.9713	2.1640	62.9642	885.7930	392.5227
P-based Reco OPF AC	2.9732	2.1564	70.5171	921.2244	433.2115
Q-based Reco OPF QCLS ⋆	2.8697	2.1543	60.1051	891.8893	387.7204
Q-based Reco OPF AC ⋆	2.8697	2.1543	60.1051	891.8893	387.7204
MVA-based Reco OPF QCLS	2.8698	2.1543	60.1104	891.9107	387.7356
MVA-based Reco OPF AC	2.8698	2.1543	60.1110	891.9107	387.7375

[1] ⋆: Best Performance.

Table 2 shows the total impact factors of all variations of the ACTIVSg200 system under different categories of contingencies. The results for *N-1* and *N-2 Generator Contingencies* are the same, and *N-1 Branch Contingencies* only have one violation with the P-based R_{ECO} using the DC power flow model. Hence, they are not included here. Among all scenarios, the Q-based R_{ECO} OPF has the best performance in terms of the severity caused by contingencies. Except *N-2 Bus Contingencies* and *N-2 Substation Contingencies*, where the P-based R_{ECO} OPF with the QCLS model and SCOPF respectively have slightly smaller impact factors, the Q-based R_{ECO} OPF has the smallest impact factors under all kinds of contingencies. The exceptions are because of P-based R_{ECO} OPF and SCOPF having more unsolved contingencies, which are worse than violations since operators cannot analyze the system. Even though the survivability of Q-based and MVA-based R_{ECO} OPFs are the same, the Q-based R_{ECO} OPF system experiences less severe disturbances and it has a higher value of R_{ECO}.

Overall, the Q-based and MVA-based R_{ECO} OPF improve the system's resilience with fewer violations and unsolved contingencies as well as less severe impacts under *N-1* and *N-2* contingencies.

6. Discussion

With the case study on the ACTIVSg200 system, the Q-based and MVA-based R_{ECO} OPF exhibit superior ability to tolerate disturbances and maintain system functionality. This was not observed from previous P-based R_{ECO} OPF or traditional OPF and SCOPF problems. The operational cost of Q-based and MVA-based R_{ECO} OPF are smaller than P-based R_{ECO} OPF but slightly higher than OPF and SCOPF (2.3%). The enhanced resilience may justify the increased operational cost. However, it is important to recognize that comprehensive contingency analysis is essentially a *preview* analysis tool to evaluate the system on all possible outages. The expected benefits from R_{ECO} OPF are uncertain, which may limit its application in the field. It is important to acknowledge that there is no way to make power systems completely invulnerable to outages National Academies of Sciences, Engineering, and Medicine (2021). Remedial actions and restoration preparations are essential in power system planning and operation. This raises a question for stakeholders: whether to operate power systems more resiliently with increased operational cost, take the risk of potential disastrous events to operate the system at its economic margin, or invest in technologies and resources to better predict risks and efficiently restore the system after disruptions.

Regarding the metric R_{ECO}, it has significant capability to account for the presence of interruptions with the information theory based formulation, especially when multiple contingencies happen. It is quite interesting to find out that the Q-based R_{ECO} OPF does not improve the Q-based R_{ECO} but instead improves the P-based and MVA-based R_{ECO}. And the Q-based R_{ECO} OPF has the highest P-based and MVA-based R_{ECO} with the best resilience under *N-1* and *N-2* contingencies.

On one hand, above outcomes emphasize the importance of optimizing reactive power flows' distribution for power systems' inherent resilience. Even though real power flows dominate power systems, reactive power flows are essential to support and stabilize the system. Due to the model complexity and economic incentives, real power based optimization models are used more in practice. Consequently, the impacts of reactive power may be overlooked. Real and reactive power are actually coupled. Reactive power flow distribution deserves more attention to be investigated for greater resilience. This calls for the development of a new pricing mechanism for reactive power generation and consumption, taking into account its influence on real power flow distribution.

On the other hand, the mathematically optimal R_{ECO} may not align with the *best* R_{ECO} for power systems. Figure 6 shows the comparison of R_{ECO} of 38 robust food webs and all variations of the ACTIVSg200 system. Resilient food webs exhibit a unique balance between network's pathway efficiency and pathway redundancy, resulting in their R_{ECO} values falling into the range of *"Window of Vitality"* Ulanowicz et al. (2009). In contrast, R_{ECO} of all ACTIVSg200 cases are out of that range. Food webs are more densely connected compared to real power grids. Although the power flow distribution can be optimized through control vectors, the limitation on network properties cannot be easily overcome with a more robust power flow distribution alone to achieve a food web's robustness. It will be of significant interests to decouple the topological properties and power flow distributions to determine a power systems' resilience metric for assessing its resilience and guide its operation for enhanced inherent resilience.

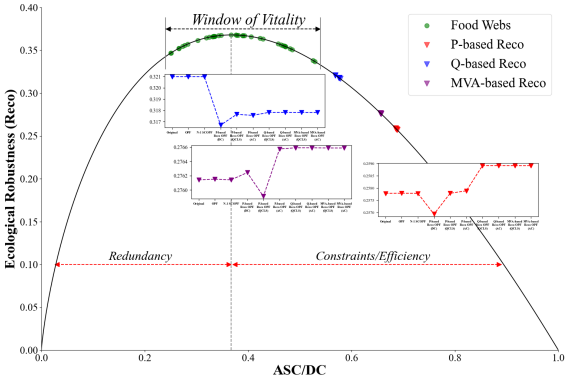

Figure 6. R_{ECO} for all variations of ACTIVSg200 cases and 38 food webs.

7. Conclusion and Future Work

Power flow distribution plays a crucial role in the inherent resilience of power systems. This paper has reformulated the R_{ECO} OPF problem with the incorporation of reactive power. Two new R_{ECO} OPFs, namely the Q-based R_{ECO} OPF and MVA-based R_{ECO} OPF, have been proposed to guide the distribution of reactive and apparent power flows, thereby enhancing power systems' inherent resilience. The Q-based R_{ECO} OPF uses reactive power flows to formulate power systems' R_{ECO}, and the MVA-based R_{ECO} OPF uses apparent power flows. Both R_{ECO} OPF problems have been applied to the ACTIVSg200 system and compared with OPF, SCOPF and P-based R_{ECO} OPF in terms of their resilience against *N-1* and *N-2* contingencies. From the case study on the ACTIVSg200 system, the Q-based R_{ECO} OPF has exhibited the best resilience, characterized by a minimal number of violations and unsolved contingencies, as well as a reduction in the severity of violated contingencies. This shows the benefit and importance of including reactive power flow in R_{ECO} to strategically guide the distribution of both real and reactive power for enhancing power systems' inherent resilience.

With analyses of different types of R_{ECO}, power flow distributions, and cost-effectiveness in enhancing resilience, three key areas warrant further investigation. First of all, it is important to establish a pricing mechanism for reactive power accounting its merit of supporting power systems and contributing to a more robust power flow distribution. This also necessitates the development of fast and reliable solvers for power system optimization problems using non-DC power flow models. Secondly, enhancing power systems' resilience inevitably entails more investment in operation and/or construction. The question remaining for stakeholders is how to trade off among the increased operational cost, the *potential* risk and cost of unexpected contingencies, and the investment in remedial actions and restoration preparations. Last but not least, R_{ECO} demonstrates its merits of quantifying a system's robustness and its ability to account for the presence of interruptions. Considering distinct characteristics of power systems, it would be of significant interest to develop a resilience metric leveraging **surprisal**, **indeterminacy**, and system **topology** for power systems to assess and guide system operation.

Acknowledgment

The authors would like to acknowledge the National Science Foundation under Grants 1916142, 2039716 and 2220347, a grant from the C3.ai Digital Transformation Institute, and the US Department of Energy Cybersecurity for Energy Delivery Systems program under Award DE-OE0000895 for their support of this work.

References

Birchfield, A. B., Xu, T., Gegner, K. M., Shetye, K. S., & Overbye, T. J. (2017). Grid structural characteristics as validation criteria for synthetic networks. *IEEE Transactions on Power Systems*, *32*(4), 3258–3265.

Cain, M. B., O'neill, R. P., Castillo, A., et al. (2012). History of optimal power flow

and formulations. *Federal Energy Regulatory Commission*, *1*, 1–36.

Capitanescu, F., Ramos, J. M., Panciatici, P., Kirschen, D., Marcolini, A. M., Platbrood, L., & Wehenkel, L. (2011). State-of-the-art, challenges, and future trends in security constrained optimal power flow. *Electric Power Systems Research*, *81*(8), 1731–1741.

Coffrin, C., Bent, R., Sundar, K., Ng, Y., & Lubin, M. (2018). Powermodels.jl: An open-source framework for exploring power flow formulations. *Proceedings of the 2018 Power Systems Computation Conference (PSCC)*, 1–8.

Glover, J. D., Sarma, M., & Overbye, T. (2012). *Power System Analysis and Design* (5th). Cengage Learning.

Huang, H., Davis, K. R., & Poor, H. V. (2023). An extended model for oobustness to capture power system resilience. *Proceedings of the 2023 IEEE PES General Meeting*, 1–5.

Huang, H., Kazerooni, M., Hossain-McKenzie, S., Etigowni, S., Zonouz, S., & Davis, K. (2019). Fast generation redispatch techniques for automated remedial action schemes. *Proceedings of the 2019 20th International Conference on Intelligent System Application to Power Systems (ISAP)*, 1–8.

Huang, H., Mao, Z., Layton, A., & Davis, K. R. (2022). An ecological robustness oriented optimal power flow for power systems' survivability. *IEEE Transactions on Power Systems*, *38*(1), 447–462.

Huang, H., Mao, Z., Panyam, V., Layton, A., & Davis, K. R. (2023). Ecological robustness-oriented grid network design for resilience against multiple hazard. *IEEE Transactions on Power Systems*, Early Access.

Kamruzzaman, M., Duan, J., Shi, D., & Benidris, M. (2021). A deep reinforcement learning-based multi-agent framework to enhance power system resilience using shunt resources. *IEEE Transactions on Power Systems*, *36*(6), 5525–5536.

Kezunovic, M., & Overbye, T. J. (2018). Off the beaten path: Resiliency and associated risk. *IEEE Power and Energy Magazine*, *16*(2), 26–35.

Kröger, O., Coffrin, C., Hijazi, H., & Nagarajan, H. (2018). Juniper: An open-source nonlinear branch-and-bound solver in Julia. *Proceedings of the International Conference on the Integration of Constraint Programming, Artificial Intelligence, and Operations Research*, 377–386.

National Academies of Sciences, Engineering, and Medicine. (2017). *Enhancing the Resilience of the Nation's Electricity System*. The National Academies Press.

National Academies of Sciences, Engineering, and Medicine. (2021). *The Future of Electric Power in the United States*.

Overbye, T. J., Vittal, V., & Dobson, I. (2012). Engineering resilient cyber-physical systems. *Proceedings of the IEEE Power & Energy Society General Meeting 2012*.

Panyam, V., Huang, H., Davis, K., & Layton, A. (2019). Bio-inspired design for robust power grid networks. *Applied Energy*, *251*, 113349.

Shaker, A., Safari, A., & Shahidehpour, M. (2021). Reactive power management for networked microgrid resilience in extreme conditions. *IEEE Transactions on Smart Grid*, *12*(5), 3940–3953.

Shield, S. A., Quiring, S. M., Pino, J. V., & Buckstaff, K. (2021). Major impacts of weather events on the electrical power delivery system in the united states. *Energy*, *218*, 119434.

Singer, B., Pandey, A., Li, S., Bauer, L., Miller, C., Pileggi, L., & Sekar, V. (2022). Shedding light on inconsistencies in grid cybersecurity: Disconnects and recommendations. *Proceedings of the 2023 IEEE Symposium on Security and Privacy (SP)*, 554–571.

Sundar, K., Nagarajan, H., Misra, S., Lu, M., Coffrin, C., & Bent, R. (2018). *Optimization-based bound tightening using a strengthened qc-relaxation of the optimal power flow problem*. arXiv preprint arXiv:1809.04565.

Ulanowicz, R. E. (1980). An hypothesis on the development of natural communities. *Journal of Theoretical Biology*, *85*(2), 223–245.

Ulanowicz, R. E. (2012). *Growth and Development: Ecological Phenomenology*. Springer Science & Business Media.

Ulanowicz, R. E., Goerner, S. J., Lietaer, B., & Gomez, R. (2009). Quantifying sustainability: Resilience, efficiency and the return of information theory. *Ecological Complexity*, *6*(1), 27–36.

Ulanowicz, R. E., & Norden, J. S. (1990). Symmetrical overhead in flow networks. *International Journal of Systems Science*, *21*(2), 429–437.

Wächter, A., & Biegler, L. T. (2006). On the implementation of an interior-point filter line-search algorithm for large-scale nonlinear

programming. *Mathematical Programming*, *106*(1), 25–57.

Zhang, W., Li, F., & Tolbert, L. M. (2007). Review of reactive power planning: Objectives, constraints, and algorithms. *IEEE Transactions on Power Systems*, *22*(4), 2177–2186.